



Action spectroscopy of a protonated peptide in the ultraviolet range

Journal:	<i>Physical Chemistry Chemical Physics</i>
Manuscript ID:	CP-ART-10-2014-004762.R1
Article Type:	Paper
Date Submitted by the Author:	17-Dec-2014
Complete List of Authors:	Canon, Francis; Synchrotron SOLEIL, ; INRA, Centre des Sciences du Goût et de l'Alimentation (UMR1324) Milosavljević, Aleksandar; Institute of Physics Belgrade, Laboratory for atomic collision processes Nahon, Laurent; Synchrotron SOLEIL, Giuliani, Alexandre; Synchrotron SOLEIL, ; Institut National de la Recherche Agronomique (INRA), Cepia

ARTICLE

Action spectroscopy of a protonated peptide in the ultraviolet range

Cite this: DOI: 10.1039/x0xx00000x

Francis Canon,^{a,b} Aleksandar R. Milosavljević,^c Laurent Nahon^a and Alexandre Giuliani^{*a,d},Received 00th January 2012,
Accepted 00th January 2012

DOI: 10.1039/x0xx00000x

www.rsc.org/

Abstract. Action spectroscopy of substance P, a model undecapeptide, has been probed from 5.2 eV to 20 eV. For photon energy above the ionization threshold measured at 10.3 ± 0.1 eV, the radical cation is observed along with side chain losses and abundant formation of all kind of sequence ions. Below the photoionization threshold, the photoproducts involve side chain cleavages and backbone cleavages into *a*-, *b*-*ly*-, and *c*- sequence ions. Different electronic excited states appear to produce different fragment ions. Norrish type I and II reactions are proposed to account for some photoproducts. This study bridges the gap between laser activation and electron-induced dissociation of peptides. Moreover, our results report for the first time a comprehensive picture of the photochemical fragmentation of a gas phase peptide in a wide photon energy range.

Introduction

The electronic structure of atoms and molecules is a property of fundamental importance in chemistry.¹ Usually, electronic structure is determined through the interplay of theory and electronic spectroscopies. The latter is ideally performed for species isolated in the gas phase, free of any external perturbations. However, both theoretical and experimental approaches are rapidly limited when the size of the species of interest grows.²

With the advent of the so-called modern ionization techniques, mass spectrometry (MS) has been granted with the possibility to manipulate larger species than previously. However, spectroscopic study on ionic targets is not a trivial task. Indeed, it is extremely difficult to measure the tiny attenuation of a beam of light passing through the low densities achievable for confined ions in the gas phase. Hence, action spectroscopy, which consists in monitoring the consequences of photon irradiation on the mass spectra as a function of the wavelength, is much more practicable and is now the basis of infrared, visible and ultraviolet spectroscopies of selected ions in the gas phase.^{3,4} These particularities have conducted pioneers to probe the spectroscopic properties of ions stored in ions traps.^{3,5} Since a vast amount of biomolecules appears under ionic form in solution, the study of the electronic properties of these species is particularly relevant. In addition, the fragmentation of polypeptide ions produced upon ultraviolet photon activation at discrete wavelength have shown very promising applications in proteomics.^{6,9}

We report herein a study of the action spectroscopy of a protonated peptide (Substance P) probed in the 5.2 eV (238 nm) to 20 eV (62 nm) photon energy range, covering continuously all previously investigated ranges. Substance P (Arg-Pro-Lys-Pro-Gln-Gln-Phe-Phe-Gly-Leu-Met-NH₂) is a model system that has been studied by many activation methods in the gas phase.¹⁰⁻¹⁷ The ionization energy of this peptide is reported and its photodissociation pathways are analyzed in terms of backbone dissociation and neutral losses. The nature of the fragmentations appears to be extremely sensitive to the chromophores probed as well as to the electronic excited states of the peptide populated upon photoabsorption. The present work provides a deeper understanding of the action of ultraviolet photons on polypeptide ions and evidences of selective photochemistry.

In a pioneer tandem time of flight (ToF) study, Barbacci and Russel¹⁴ have found that activation of Substance P singly protonated ion gave rise only to *a*- and *d*- sequence ion series. Subsequently, this group has reinvestigated photon activation of Substance and found a different fragmentation pattern, highlighting the effect of the matrix nature on the tandem mass spectra.¹⁹ Cui *et al.*¹² have reported that upon photon activation at 157 nm in tandem ToF experiment, Substance P produced abundant series of *a*- and *d*- sequence ions, with *c*₂- and *b*₂- fragments. Moon *et al.* have observed under 193 nm photon activation also in tandem ToF the same *ald*- fragment ion series along with a *c*₆- ion. In a subsequent studies at the same photon activation wavelength,²⁰ this group has confirmed the *ald*- ions, but without the *c*₆- sequence ion and with a new

series of *b*- fragments. In contrast to previous work on singly protonated peptides,²¹ identical fragmentation patterns were observed for photon activation at 193 nm and 266 nm, casting doubt on the threshold for these backbone fragmentations. The region below 157 nm, has been investigated by Bari *et al.*²² for leucine enkephaline. Their study was performed using synchrotron radiation in the 8 to 40 eV photon energy range. The fragmentation patterns appeared different below and above the ionization threshold. At low photon energy, the mass spectra were dominated by neutral losses involving tyrosine, immonium ions, and abundant *b*₃- and *y*₂- fragment ion, along with a low abundant *a*₄- ion. Their similarity to low energy collisional activation conditions of the peptide, has led to the proposition that, in the 8 to 9 eV range, photodissociation would occur following intramolecular vibrational energy redistribution. Such an interpretation differs from previous laser based studies. It is worth noting that these measurements could have been affected by higher order light. Above the ionization threshold, the fragmentation patterns changed with the appearance of sequence ions of various natures. Subsequent study on poly-glycines of increasing size has allowed the effect of the peptide chain length to be investigated. Interestingly, the patterns changed at 5 glycine residues from side chain losses to backbone *a*- and *b*- sequence ions.²³ However, the thresholds for these fragments ions were not reported. Brunet *et al.*²⁴ have reported absorption bands in the VUV for peptide polyanions. In a recent study on a small protein at some selected wavelength including 193 and 157 nm,^{4,8} different dissociation regimes were observed. Interestingly, at photon energies corresponding to 193 and 157 nm,⁸ abundant *a/x*- series were formed, with a few *b/y*- sequence ions. At higher photon energy, all kind of backbone fragmentation were observed and attributed to a dissociative photoionization regime.

Most laser based experimental studies agree on the formation of *a*- and *d*- sequence ions for singly protonated substance P, but disagree on the nature of other fragments. Higher photon energy excitation studies on other peptides have reported different fragmentation patterns. In the present work, we want to bridge the gap between laser-based experiments and other light sources and to shed light onto some inconsistencies found in the literature. To reach this goal, relative fragmentation cross sections have been measured thanks to the high spectral purity, photon energy resolution, and tunability of the synchrotron radiation beamline used here.

Material and methods

Samples

Substance P was obtained from Sigma. For MS analysis, the polypeptide was diluted to a final concentration of 10 μM in a water/acetonitrile/acetic acid (49.5:49.5:1 v/v/v) mixture.

Mass spectrometry & action spectroscopy

The experimental setup is based on the coupling of a linear ion-trap mass spectrometer (LTQ XL, Thermo Electron, San Jose, CA, USA) to the DESIRS VUV beamline at the SOLEIL synchrotron radiation facility (France),²⁵ as described in details elsewhere.²⁶ The precursor ion at *m/z* 1347 was selected and the mass spectrometer was tuned in a collision induced dissociation mode, with 5 Da isolation width, collision energy set to zero and 500 ms activation time. As can be seen in figure S1, this window selection and storage time does not induced any fragmentation without photons, beside a neutral loss. Briefly, the photon beam is injected along the ion trap axis from the back side of the spectrometer. An MgF₂ window (5.2-10 eV) and an Argon filled gas filter (8-16 eV) were used to suppress the high harmonics of the photon source (undulator) that would be transmitted by the monochromator's grating, thereby ensuring spectral purity of the incident radiation. The typical spectral bandwidth was in the 10 meV range. An electromechanical shutter was placed along the synchrotron radiation (SR) beam, allowing a precise control of the irradiation time and its synchronization with the LTQ time sequence.²⁷ The electrosprayed ions were selected and stored in the ion trap in a tandem MS (MS2) scheme, in which the activation energy was set to zero, and the activation time to about 500 ms. The photon flux, in the 10¹¹-10¹² ph/s range, was measured using a calibrated photodiode (AXUV, International Radiation Detectors) placed just before the entrance of the ions trap. The photon flux is provided in figure S2.

Data treatment

Relative partial cross sections are obtained from the recorded mass spectra by measuring the surface of the peak of an ion of interest. This abundance is then normalized to the sum of abundances of the parent ions and all the fragments. Finally, the obtained ratio are normalized to the independently measured photon flux to produce relative partial cross sections, also called normalized ion yields. Data have been analyzed using Mmass²⁸ and Igor Pro (Portland, O., USA).

Results

Action spectroscopy of a singly protonated Substance P has been probed from 5.2 eV to 20 eV photon energy. Figure 1 shows the tandem mass spectra of Substance P obtained for several characteristic photon energies, namely 6.4 eV (193 nm), 7.8 eV (158 nm), 9 eV (138 nm), 12 eV (103 nm) and 18 eV (69 nm). The photon energies investigated here cover both the photodissociation (figure 1a, 1b and 1c) and dissociative photoionization (figure 1d and 1e) regimes of the parent ion. In the following, we first pay attention to the photoionization of substance P. Then, the backbone fragmentations and the side chain losses are presented.

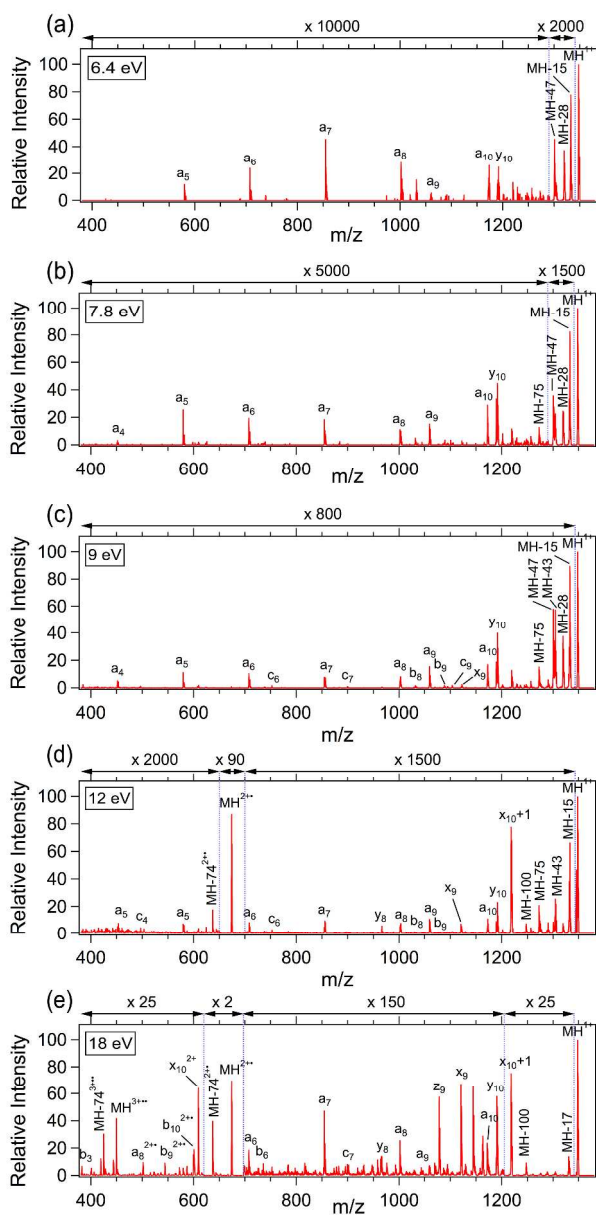


Figure 1. Photon activation mass spectra of the Substance P $[M+H]^+$ precursor ion at (a) 6.4 eV (193 nm), (b) 7.8 eV (159 nm) and (c) 9 eV (138 nm), (d) 12 eV (103 nm) and (e) 18 eV (69 nm) photon energy.

Ionization energy of Substance P

A striking feature in the mass spectrum recorded at 12 eV and above is the appearance of a product ion at m/z 673.8, which corresponds to the radical cation produced by photoionization of the precursor according to: $[M+H]^+ + h\nu \rightarrow [M+H]^{2+} + e^-$. The normalized ion abundance of $[M+H]^{2+}$ plotted as a function of the photon energy in figure 2 may be fitted to a linear threshold law in the vicinity of the threshold to extract the ionization energy (IE) of the protonated peptide.

We find a value of 10.3 ± 0.1 eV corresponding to the adiabatic IE of the singly charged cation. In their pioneering

works, Zubarev and coworkers^{10,29} have reported electron impact measurements of the ionization energies of isolated $[M+H]^+$ Substance P ions in Fourier Transform (FT) - Ion Cyclotron Resonance (ICR) instruments. The 11.0 ± 0.4 eV value derived in Ref. 29 from both MALDI and ESI measurements is slightly larger than our present result, while their ESI data²⁹ gave 10.7 ± 0.5 eV. The latter value is in agreement with the present findings within the experimental uncertainty. It is worth noting that our measurements provide IE values with an increased relative precision around 1% as compared to the 5% from electron impact data.

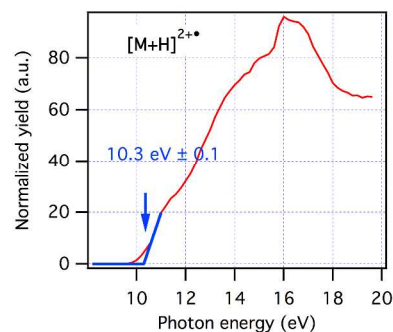


Figure 2. Normalized ion yield from the photoionization product ion $[M+H]^{2+}$ as a function of the photon energy (red curve). Fitting to a linear law (blue curve) allows extracting the ionization thresholds value of $10.3 \text{ eV} \pm 0.1$ eV for singly protonated Substance P ion, as indicated by the arrow.

In a previous study on the IE of polypeptides as a function of the charge state,³⁰ it has been proposed that the highest occupied molecular orbital of polypeptides lies on the residues with the lowest ionization energy. Theoretical calculations on leucine enkephaline protonated peptide have located the HOMO on the aromatic amino acids.³¹ Although the IE is not known for all amino acids,³² methionine is expected to have the lowest vertical IE at 8.65 eV³³ among the constitutive amino acids of Substance P. The difference between the IE of the neutral amino acid and the present (adiabatic) measurement is ascribed to the Coulombic effect of the extra charge added upon protonation. Hence, according to a previous study, this difference in the IEs can be related to the distance between the methionine and the protonation site.³⁰ The 1.65 ± 0.2 eV change in the IE corresponds to a Coulomb repulsion with a charge situated at 8.7 ± 1 Å. This experimental value compares favorably with the theoretical distance between the sulfur atom and the protonated nitrogen of the guanidine group obtained by molecular dynamic (see supplementary data, figure S3).

Above $12.9 \text{ eV} \pm 0.1$ the doubly ionized ion $[M+H]^{3+}$ is also observed in agreement with previous report from Zubarev and Yang under electron impact ionization of polypeptides.³⁴ The origin of this multiply ionized species is not clearly established and requires additional work, as it may arise from sequential ionization of the products or from direct double photoionization, as reported recently for double direct photodetachment.³⁵

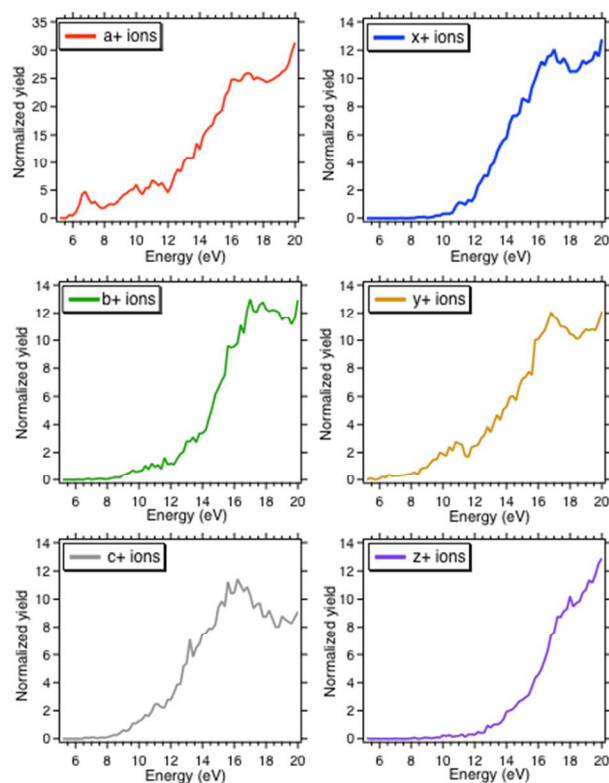


Figure 3. Normalized ion yields in arbitrary units for the sequence ions as a function of the photon energy in the 5.2 to 20 eV range.

Backbone fragmentations

Figure 1a and 1b present the photon activation mass spectra of $[M+H]^+$ ion of Substance P at 6.4 eV (193 nm) and 7.8 eV (159 nm), in order to compare the present work with the previous ones based on excimer lasers.^{6,7,36-38} For comparison a CID spectrum of singly protonated Substance P is presented in figure S4. The fragmentation patterns observed under the statistical condition of CID excitation are very different from those obtained at 6.4 and 7.8 eV. Indeed, we observed mostly ions formed upon breaking the C_{α} -N bond, accompanied by a_7 - and a_8 - fragment ions. Formation of a - sequence ions has been reported previously for Substance P at 193 and 157 nm by Reilly and coworkers using a MALDI ToF-ToF instrument and ESI linear ion trap^{12,13}. Very similar sets of a - ions are observed at both wavelengths, with abundant a -sequence ions ranging from a_4 to a_{10} . It should be noticed that the ion abundance remains very stable along that series. X - sequence ions are not detected owing to presence of an arginine, which sequesters the charge near the N-terminal part of the peptide. The origin of radical ion, such as the a_n+1 and a_n+1 , has been proposed to be linked to the presence of the glycine residue, which prevents from the β -elimination³⁷ that leads to regular a - sequence ions after homolytic bond cleavage. The y_{10} ion, which is also observed in figure 1a and 1b, has been proposed to originate from charge remote fragmentation on a hot ground state for peptide containing N-terminal arginine.^{36,37} A striking difference between the present measurements and those performed upon

laser activation is the total absence of d - sequence ions under SR activation. Note that SR is much less intense than a laser radiation of the same photon energy. Thus, these ions may originate from multiphoton effects, as a consequence of the high power delivered by the laser source. However, Thompson *et al.*¹³ have checked the effect of laser power on a small peptide for both wavelengths and reported that higher laser power improved the quality of the tandem mass spectra, without affecting much the fragmentation pattern. Additional work is therefore needed to elucidate the nature of this difference between SR and laser based activation.

At higher photon energies, new sequence ions are observed together with the previously discussed a - sequence. As seen in figure 1c, b -, and c - ions appear at 9 eV photon energy. It is worth noting that this fragmentation regime has never been reported so far.

The fragmentation patterns change drastically above the ionization threshold, as seen in figure 1d and 1e, which is in agreement with previous observation for small peptides²² and proteins.⁸ Indeed, in addition to the a - series discussed above, new x -, b -/ y -, and c -/ z - fragments appear. Moreover, doubly charged fragments of a -, b -, and x - nature are produced. Clearly new fragmentation channels open above the ionization threshold, which are certainly to be related to dissociative photoionization (DPI). Figure 3 presents the normalized backbone fragment ion yields for the observed sequence ions of Substance P as a function of the photon energy. The onset for a - ion formation is found around 5.5 eV. The a - ions yield shows clearly a band centered at 6.8 eV, followed by another one starting at 8 eV and peaking at 10 eV. B - and c - fragment ions appear above 8 eV, which explains why fragments of this nature have never been observed under excimer laser activation conditions. The same band centered on 10 eV is also observed for a -, b -, c - and y - ions. The C-terminal x - and z - fragments are detected only above the ionization threshold.

Neutral losses

Neutral losses are among the most abundant fragmentations occurring over the entire photon energy range investigated here. They mostly involve side chain fragmentations. Table 1 gathers the assignment made for all the neutral losses observed from the protonated molecule $[M+H]^+$ and the radical photoion $[M+H]^{2+}$ precursors along with the observed appearance energies. Neutral losses occurring from the protonated molecule and those accompanying photoionization of the precursor are discussed separately.

From the precursor ion

With the exception of proline and glycine, all the residues are subject to side chain losses. The assignments of the losses are made on the basis of the masses and spectral dependencies of the yields, some of which are presented in figure 4 and in figure S5. All the yields appear structured with well-resolved band for numerous side chain losses. They reveal also that these losses are differently affected by the photon wavelengths.

The only fragmentations showing abundance below 5.2 eV involve the C-S bond of the methionine: -15 Da and -47 Da, as seen in figure 4 and figure S5. This observation is in agreement with the reported $n_s\text{-}\sigma^*$ absorption band for sulfur containing amino acids in solution.³⁹ Although of low oscillator strength, these electronic transitions, are strongly dissociative along the C-S bond. These fragmentations had already been reported by Reilly and co-workers under 193 and 157 nm laser irradiation^{13,37}. Methionine has also been found to lose $\text{CH}_2\text{SCH}_3^{\cdot}$ (-61) and $\text{C}_2\text{H}_3\text{SCH}_3$ (-74 Da) upon PD,^{13,37} ECD,^{11,40} EID,^{10,41} and CID of α -radical peptides.⁴² The onsets for losses of 61 and 74 Da, which both involve C-C bond cleavage, are found at 8 eV and above 6.4 eV, respectively. We report for the first time loss of 75 Da. The fragmentation yield (figure S5) of loss of 75 Da closely is similar to that of -74 Da, which suggests assigning this loss to $\text{C}_3\text{H}_7\text{S}^{\cdot}$. Similarly, we tentatively assign the loss of 62 Da to $\text{C}_2\text{H}_6\text{S}$ from Met, on the basis of a similar photon energy spectrum as that of 61 Da.

Table 1. Neutral losses (in Da) from amino acid sides chain from the protonated molecule and from the radical cation. Appearance energies (AE) in eV, are given with ± 0.1 eV uncertainty.

Residue	Loss	Precursor			
		$[\text{M}+\text{H}]^+$		$[\text{M}+\text{H}]^{2+}$	
		Assignment	AE	Assignment	AE
Arginine	43	$\text{CH}_3\text{N}_2^{\cdot}$	6.0	$\text{CH}_3\text{N}_2^{\cdot}$	11
	44	CH_4N_2	6.0		
	72	$\text{C}_2\text{H}_6\text{N}_3^{\cdot}$	8.0		
	35	$2\text{NH}_3+\text{H}$	9.0		
	59	CH_5N_3	8.0	CH_5N_3	12.9
	87	$\text{C}_3\text{H}_9\text{N}_3$	9.5		
Lysine	100	$\text{C}_4\text{H}_{10}\text{N}_3^{\cdot}$	8.0		
	16			NH_2^{\cdot}	12.1
	17	NH_3	8.0	NH_3	12.1
Glutamine	73	$\text{C}_4\text{H}_{10}\text{N}^{\cdot}$	6.4		
	43			$\text{CH}_3\text{N}_2^{\cdot}$	11
	45	CONH_3	5.5	CONH_3	11
Phenylalanine	58			$\text{C}_2\text{H}_4\text{NO}^{\cdot}$	12.2
	91	$\text{C}_7\text{H}_7^{\cdot}$	8.0	$\text{C}_7\text{H}_7^{\cdot}$	12.1
	Leucine	43	C_3H_7	6.0	C_3H_7
56				C_4H_8	12.2
58				$\text{C}_2\text{H}_8\text{N}$	12.2
Methionine	15	CH_3^{\cdot}	< 5.2	CH_3^{\cdot}	12.4
	47	$\text{CH}_3\text{S}^{\cdot}$	< 5.2	$\text{CH}_3\text{S}^{\cdot}$	11
	61	$\text{C}_2\text{H}_5\text{S}^{\cdot}$	8.0	$\text{C}_2\text{H}_5\text{S}^{\cdot}$	13
	62	$\text{C}_2\text{H}_6\text{S}$	8.0		
	74	$\text{C}_3\text{H}_6\text{S}$	6.4	$\text{C}_3\text{H}_6\text{S}$	12.3
	75	$\text{C}_3\text{H}_7\text{S}^{\cdot}$	6.1		
N-term	91	$\text{C}_3\text{H}_6\text{S}+\text{NH}_3$	8.0		
	16			NH_2^{\cdot}	12.1
C-term	17	NH_3	8.0	NH_3	12.1
	45	CONH_3	5.5	CONH_3	11
Unknown	28	CO	5.5		
	29	$\text{CO}+\text{H}$	5.5	$\text{CO}+\text{H}$	12.4

Loss of 91 Da has been observed under ECD condition and assigned to $\text{C}_3\text{H}_6\text{S}+\text{NH}_3$ from Met,⁴⁰ but its photon energy spectrum is very different from that of loss 74 Da. This fragmentation channel could also come from the loss of C_7H_7 from Phe. Loss of 45, also reported under ECD conditions, has been assigned to CONH_3 from Gln. The corresponding ion yield shows a rather sharp feature peaking at 6.8 eV (182 nm). This wavelength match nicely the absorption band attributed to $\pi\pi^*$ transitions involving the Gln side chain,³⁹ which adds credence to the interpretation. Loss of 44 Da has also been observed following ECD and assigned to CH_4N_2 from Arg. The corresponding ion yield also exhibits sharp features in the low photon energy range, peaking at 7 eV. In solution, $\pi\pi^*$ transitions of Arg have been found at 177 nm (7 eV), again in excellent agreement with the present 7 eV observation. Loss of 43 Da has been suggested to arise from Leu (C_3H_7) and Arg ($\text{CH}_3\text{N}_2^{\cdot}$), based on previous assignments. The ion yields associated with this loss shows a peak at 7.1 eV, which match the transition of the $\pi\pi^*$ feature observed for Arg in solution.³⁹ However, the involvement of Leu in this loss cannot be ruled out as it could contribute to the ion yield at higher photon energy.

From the radical cation

Similarly to the case of the singly protonated molecular ion, neutral losses from the radical cation involves all amino acids, with the exception of glycine and proline, as seen in Table 1. The neutral losses accompanying the $[\text{M}+\text{H}]^{2+}$ radical cation are produced very likely upon dissociative photoionization (DPI) of the $[\text{M}+\text{H}]^+$ precursor. Indeed, loss of 47 Da (CH_3S from methionine) is found with low appearance energy of 11 ± 0.1 eV in figure S6 that is 0.7 eV above the ionization threshold. This value is consistent with the HOMO sitting on the methionine residue. Other losses from methionine corresponding to CH_3 (15 Da), $\text{C}_2\text{H}_5\text{S}$ (61 Da) and $\text{C}_3\text{H}_6\text{S}$ (74 Da) show up above 12.4 eV, 13 eV and 12.35 eV respectively. Loss of 43 Da, assigned to C_3H_7 (leucine) or CH_3N_2 (arginine) appears above 11 eV. Arginine is the residue on the peptide having the second lowest ionization energy.³² Slightly higher in energy (11.0 ± 0.1 eV) appears the loss CONH_3 (-45 Da) from glutamine or from the C-terminal amide. To our knowledge, no data have ever been reported on the ionization energy of glutamine. However, the ionization energy of acetamide has been measured at 9.71 ± 0.02 eV,⁴³ which is above all the other chromophores of Substance P, except glycine.³² Hence, it is likely that loss of 43 Da is due to glutamine. Losses of 16 Da (NH_2) and 17 Da (NH_3), assigned either to N-terminal or to lysine, appear at 12.1 ± 0.1 eV. Also at 12.1 eV the loss of 91 is observed, which may be assigned to C_7H_7 from phenylalanine or to $\text{C}_3\text{H}_6\text{S}+\text{NH}_3$ from methionine. However, the appearance energy of $\text{C}_3\text{H}_6\text{S}$ (74 Da) is measured at 12.3 ± 0.1 eV, which is higher in energy. It is unlikely that loss of $\text{C}_3\text{H}_6\text{S}+\text{NH}_3$ exhibit lower appearance energy than that of C_3H_6 , which lead us to assign the loss of 91 Da to C_7H_7 for phenylalanine. Slightly above in energy, losses of 56 Da (C_4H_8) and 58 Da (NH_2COCH_2 or $\text{C}_2\text{H}_8\text{N}$) found at 12.2 ± 0.1 eV and are assigned to leucine,

glutamine or lysine, respectively. Loss of 59 Da from arginine is assigned to CH_5N_3 with appearance energy of 12.9 eV. Losses of 16 Da (NH_2), 47 Da (CH_3S), 56 Da (C_4H_6) and 58 Da (NH_2COCH_2 , $\text{C}_2\text{H}_6\text{N}$) are observed only from the radical cation $[\text{M}+\text{H}]^{2+}$. It is worth noting that fewer neutral losses from the radical cation have been reported for substance P under EID activation conditions.¹⁰ Indeed, only losses of 74 Da, 61 Da and 16 Da had been observed, although EID and DPI are very similar in their physical process.

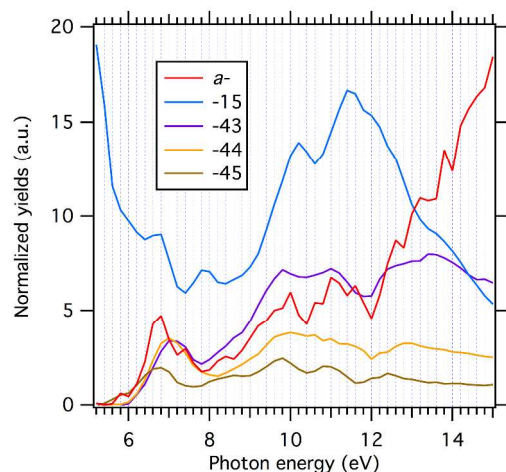


Figure 4. Normalized yields for characteristic neutral losses (in Da) from the $[\text{M}+\text{H}]^+$ precursor ion and α -sequence ions in the 5.2 – 15 eV

Discussion

The electronic spectroscopy of small peptides has been extensively studied both theoretically and experimentally. However, this is the first time that photodissociation of a gas phase peptide is explored over such a wide photon energy range, spanning nearly from the absorption onset up to several eV above the ionization threshold. Previous studies have focused mostly on the near UV range with some excursion in the VUV using laser lines.^{9,21,36,38-47} Our measurements lead us to propose a tentative rationalization of the photochemistry of peptides, summarize in figure 5. The observed fragmentation yields arise from the convolution of the photoabsorption cross section of the precursor with the fragmentation efficiency and relaxation pathways of the particular excited state populated. Interestingly, the spectral features observed in figure 3 and 4 correspond nicely with those observed in the photodetachment yield of doubly deprotonated peptides.²⁴

The spectral region above 250 nm (below 4.96 eV) is ascribed mostly to $\pi_a\pi_a^*$ electronic transitions involving the aromatic amino acids and to a lesser extent to $\pi_c\sigma^*$.⁴⁸⁻⁵¹ The photochemistry of small peptides containing aromatic residues has been probed at 266 nm,⁴⁴ 263 nm,^{45,46} and at 260 and 220 nm²¹ by laser activation. Perot *et al.*⁴⁵ have proposed a rationalization of the fragmentations of di- and tripeptides in which the promoted electron, referred to as the active electron,

drives the fragmentations. At these wavelengths, excitation of an electron from the aromatic π_a orbital to an unoccupied orbital localized near the aromatic group are involved. The most abundant fragmentations following photon excitation of aromatic amino acids involve side chain losses. Low abundant backbone cleavages have been observed, and suggested to occur on hot ground electronic state after internal conversion (IC).¹³

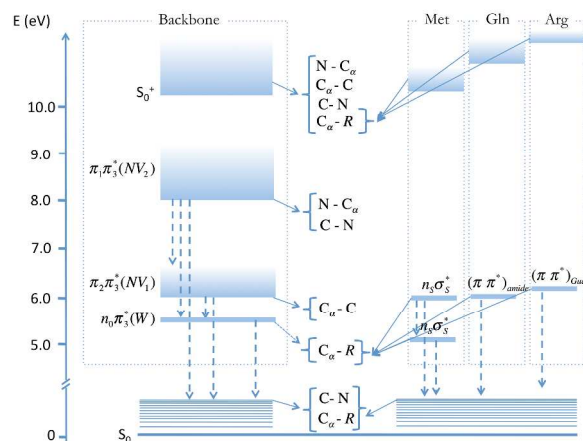


Figure 5. Energy diagram for substance P showing the different chromophores: the backbone, Met, Arg and Gln. The dissociations occurring from the electronic levels are indicated by the blue arrows. Non radiative decays are indicated by the dashed arrows.

Although the aromatic residues have been found to contribute at higher photon energy, at 6.4 eV most of the photoabsorption cross section comes from transitions involving the peptidic backbone.⁵²⁻⁵⁴ The peptidic bond has been described as a four level system in di- and tripeptides, involving two occupied π orbitals (π_1 and π_2), the oxygen lone pair n_o and the virtual π_3^* orbital. The π_1 , π_2 and π_3^* orbitals involve the peptidic bond and have been found to be bonding, non-bonding, and anti-bonding in nature, respectively, for model amides and peptides.^{55,56} The 191 nm (6.5 eV) absorption band reported for protein and peptide in solution^{57,58} is assigned to the $\pi_2\pi_3^*$ (NV_1) transition. The $n_o\pi_3^*$ (W) transition is found around 5.5 eV (225 nm) but has a weak oscillator strength. Charge transfer transitions involving neighboring amino acids have been suggested to give rise to feature around 7.5 eV (165 nm).^{54,59} The $\pi_1\pi_3^*$ transition has been proposed to be account for the 9.5 eV (130.5 nm) band.⁵³

Figure 4 compares the normalized ion yields for α -sequence ions along with those for loss of 15, 43, 44 and 45. As mentioned above, the loss of 15 Da involves the sulfur photoabsorption manifold. Goto *et al.*³⁹ have measured the absorption spectra of individual amino acids in solution from 300 nm (4.1 eV) to 145 nm (8.55 eV) and reported the specific contributions of side chains in that range. The absorption tail for alkyl sulfides extends slightly below 230 nm (5.4 eV).^{39,60} Our data show extensive fragmentations of the $\text{S}-\text{CH}_3$ and CH_2-S bonds already at 5.2 eV, see figure 4, which decrease with

increasing photon energy. A feature is observed in figure 4 at 6.8 eV (182.3 nm), which could correspond to the second $n_s\sigma^*$ transition observed for isolated alkyl sulfides^{60,61} or to the peptide $\pi_2\pi_3^*$ transition, since this feature match very well the maximum of the a^- ion yield, which has been assigned to the NV1 transition (see below). Yields for losses of 43 Da, 44 Da and 45 Da possess a maximum at 7.2 eV, 7.2 eV and 6.8 eV. These neutral losses have been assigned to Arg or Leu for 43, to Arg for 44 and to Gln. However, the spectral feature at 7.2 and 6.8 eV is indicative of $\pi\pi^*$ transitions related to Arg or Gln. The Gln band match nicely the amide NV1 features observed in the a^- ion yield in figure 4. The $\pi\pi^*$ transition for Arg involves the guanidinium group and thus appears at higher photon, in agreement with the observation of Goto *et al.*³⁹ who finds the transition at 177 nm for Arg and 183 nm for Gln. Hence the ion yields for neutral losses show features characteristic of the absorption manifold of the chromophores of individual amino acids, which appear to be decoupled from the others. This is represented in the energy diagram in figure 5, where the energy levels for alkyl sulfide of Met and those for Gln and Arg give rise to neutral losses.

Formation of a^- sequence ions has been proposed by Thompson *et al.*⁶² to arise from a Norrish I reaction after homolytic cleavage the $C_\alpha-C$ bond and H• elimination. Recently, Parthasarathi *et al.*⁴⁷ have revisited theoretically the photochemistry of small peptides at 157 nm excitation. It has been proposed that 157 nm excitation populated a Rydberg state.

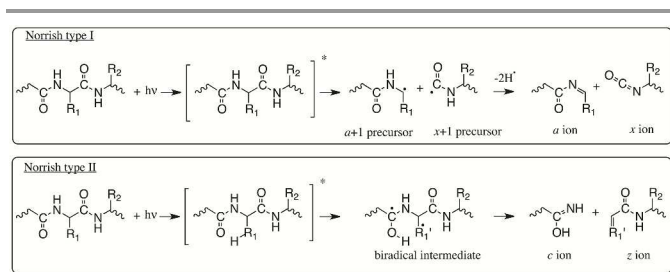


Figure 6. Norrish type I and type II photochemical reactions leading to the formation of a/x^- and c/z^- sequence ions, respectively.

Since Rydberg states converge towards the ionic limit, the effect of the removal of an electron on dialanine peptides has been investigated. The ionization has been found to affect severely the $C_\alpha-C$ bond strength and thus Rydberg excitation has been suggested to be a possible origin for a^-/x^- ions. The present measurement has been made with photon energy steps too large to detect Rydberg states, which usually present sharp excitations.⁶³ However, our observations do not support this exclusive Rydberg states origin of fragmentation. Indeed, the a^- ion yield in figure 3 is structured and shows a band peaking around 6.8 eV, which matches nicely with the energy of $\pi_2\pi_3^*$ (NV1) transition. Hence, we propose that following NV1 transition, $C_\alpha-C$ bond cleavage occurs through a Norrish I type reaction, as figured in the energy diagram in figure 5 and according to the scheme in figure 6. Note that the proposed Norrish type I mechanism is different from that proposed by

Reilly¹² and Yoon.²⁰ Indeed, as we did not observed any d^- sequence ions, we proposed that H-loss occur from the backbone and not from the side chain. The NV1 state may also decay to the W state, which does not produce backbone fragmentations.⁴⁵ However, formation of y_{10}^- sequence ion at 6.4 eV (figure 1) would occur from a hot ground state following non-radiative decay as suggested earlier,¹³ which is another possible decay from NV1 and is sketched in figure 5. At 8 eV, other channels open for backbone fragmentations (as seen in figure 3), with the appearance of b^-/y^- and c^- fragments. Spectroscopic measurements in this VUV region are very rare for peptides. For amides, the corresponding state $\pi_2\pi_3^*$ (NV2) has been suggested to partly relax down to the singlet or triplet $\pi_2\pi_3^*$ (NV1) through IC or ISC, respectively, and to produce $C_\alpha-C$ bond cleavages.⁶⁴ This mechanism may accounts for the formation of a^- ions above 8 eV, as seen in figure 5. However, it does not hold for the other bond cleavage observed leading to b^-/y^- and c^- sequence ions. Formation of b^- and y^- sequence ions might occur either from a hot ground state following non-radiative decay or from the NV2 electronic excited state, through a Norrish I reaction scheme (figure 6). In the same mind, the c^- ions are very likely formed from the electronic excited NV2 states. A possible formation mechanism could involve a Norrish II reaction, as depicted in figure 6.

Upon photoionization an additional charge is created somewhere on the precursor ion, which leads to fragmentation of the backbone and side chain and makes detection of C^- terminal ion series possible. Neutral losses are abundant after photoionization. Different appearance energies are observed for losses corresponding to different amino acids. We suggest that photoionization of specific amino acid occurs at a particular photon energy that matches the ionization energy of the residue augmented by an additional value created by the Coulomb attraction due to the protonation. Photoionization of each amino acid may lead to a rapid side chain loss, as indicated in figure 5. Electron ionization dissociation (EID) of Substance P has been reported by the Zubarev group.¹⁰ The fragmentation patterns produced here upon DPI and those from EID activation conditions appear very similar. Both methods enhance the abundance and the diversity of fragments. Kalcic and coworkers in their femtosecond laser induced dissociation (fs-LID) study of protonated peptides^{65,66} have reported full sequence coverage from numerous a^-/x^- , b^-/y^- and c^-/z^- fragments. The fs-LID process is initiated by tunneling ionization which produces a $[M+H]^{2+}$ radical cation. Hence, EID,¹⁰ fs-LID^{65,66} and dissociative photoionization (DPI) are similar in nature, relying on the same physics. The radical cation generated by these activation methods is subject to proton and radical directed fragmentation and generates abundant sequence ions of all nature. These characteristics are valuable for proteomic analysis, as reported by Canon and coworkers.⁸ Interestingly, Laskin and collaborators⁶⁷ have observed abundant formation of a^- sequence ions and side chain losses upon CID activation of radical $[M+H]^{2+}$ peptides. However, they did not observe the variety of sequence ions reported here. This clearly indicates that radical peptide ions

produced by homolytic bond cleavage upon CID excitation⁶⁷ differs in nature from the radical cation produced by ionization.

Conclusions

Action spectroscopy of isolated protonated substance P cation has been probed in the 5.2 to 20 eV range using synchrotron radiation. The ionization energy of the cation is measured at 10.3 ± 0.1 eV in agreement with previous electron impact data.

Three fragmentations regimes are clearly identified. Above the ionization threshold, abundant fragmentations into all sequence ions are produced. This dissociative photoionization (DPI) regime is similar in nature to the fs-LID and to EID activation conditions. Below the ionization threshold, photodissociation takes place. The spectral region investigated here covers for the first time non-localized electronic excitations involving the amide bond. The fragmentation yields as function of the photon energy show features that could be assigned to known electronic excited states already described for polypeptides. It appears that the W, NV1 and NV2 excited states possess different photochemistry giving rise to product ions of different nature. Norrish type I and II reactions are tentatively suggested to account for the observed backbone fragmentation. Additional theoretical and experimental works are needed to provide deeper insight into the photochemistry of higher excited states of peptides and proteins. Nevertheless, the wide photon energy range covered in this study allows bridging the gap between different excitation conditions, such as LID at 193 and 157 nm, EID and fs-LID.

The present work also demonstrates that photochemistry of isolated peptides is highly selective. First, the photochemistry of the peptide appears to be sum of the photochemistry of all individual chromophores, which may be categorized into side chains and peptidic backbone. Energy deposition into excited state involving side chains lead to neutral losses and not to backbone cleavage. Conversely, photoabsorption by the peptide amides bond leads to backbone cleavages. Interestingly, action spectroscopy allows sorting out the photochemistry of specific absorbers by looking at particular fragments. Second, chemical selectivity also occurs as a function of the photon energy. Interestingly, photon excitation on the NV1 peptide state produces a very different fragmentation pattern than higher excited states involving the backbone.

The fragmentations are abundant, even at low photon energy. The spectral region below 7.6 eV (163 nm) is of great interest in structural biology, as it is a region probed by circular dichroism for the elucidation of the secondary structure content of polypeptides. Degradation under VUV synchrotron radiation exposure of proteins is an interesting process for a large community⁶⁸.

Acknowledgements

‡This work was supported by the Agence Nationale de la Recherche, France, under project ANR-08-BLAN-0065. A.R.M. acknowledges support by the Ministry of Education, Science and technical development of Republic of Serbia (Projects No. 171020). The SOLEIL synchrotron radiation facility is acknowledged for providing beamtime under project 20090862.

Notes and references

^a *Synchrotron SOLEIL, l'Orme des Merisiers, St Aubin, BP48, 91192 Gif sur Yvette Cedex, France*

^b *UMRI324 Centre des Sciences du Goût et de l'Alimentation, INRA, F-21000 Dijon, France*

^c *Institute of Physics Belgrade, University of Belgrade, Pregrevica118, 11080 Belgrade, Serbia*

^e *UAR1008, Cepia, INRA, BP 71627, 44316. ; E-mail: giuliani@synchrotron-soleil.fr*

Electronic Supplementary Information (ESI) available. See DOI: 10.1039/b000000x/

1. K. Fukui, *Angew Chem Int Ed Engl*, 2003, **21**, 801–809.
2. R. Weinkauff, J. P. Schermann, M. S. de Vries, and K. Kleinermanns, *The European Physical Journal D*, 2002, **20**, 309–316.
3. T. Baer and R. C. Dunbar, *Journal of the American Society for Mass Spectrometry*, 2010, **21**, 681–693.
4. A. Giuliani, A. R. Milosavljević, F. Canon, and L. Nahon, *Mass spectrometry Reviews*, 2014, **33**, 424–441.
5. R. Dunbar, *International Journal of Mass Spectrometry*, 2000, **200**, 571–589.
6. J. A. Madsen, D. R. Boutz, and J. S. Brodbelt, *J. Proteome Res.*, 2010, **9**, 4205–4214.
7. L. Zhang and J. P. Reilly, *J. Proteome Res.*, 2010, **9**, 3025–3034.
8. F. Canon, A. R. Milosavljević, G. van der Rest, M. Réfrégiers, L. Nahon, P. Sarni-Manchado, V. Cheynier, and A. Giuliani, *Angewandte Chemie International Edition*, 2013, **52**, 8377–8381.
9. J. S. Brodbelt, *Chemical Society Reviews*, 2014, **43**, 2757–2783
10. Y. M. E. Fung, C. M. Adams, and R. A. Zubarev, *J. Am. Chem. Soc.*, 2009, **131**, 9977–9985.
11. J. Axelsson, M. Palmblad, K. Håkansson, and P. Håkansson, *Rapid Communications in Mass Spectrometry*, 1999, **13**, 474–477.
12. W. Cui, M. S. Thompson, and J. P. Reilly, *Journal of the American Society for Mass Spectrometry*, 2005, **16**, 1384–1398.
13. M. Thompson, W. Cui, and J. Reilly, *Journal of the American Society for Mass Spectrometry*, 2007, **18**, 1439–1452.
14. D. Barbacci and D. Russell, *Journal of the American Society for Mass Spectrometry*, 1999, **10**, 1038–1040.
15. D. Debois, A. Giuliani, and O. Laprévotte, *Journal of Mass Spectrometry*, 2006, **41**, 1554–1560.
16. V. Larraillet, A. Vorobyev, C. Brunet, J. Lemoine, Y. O. Tsybin, R. Antoine, and P. Dugourd, *Journal of the American Society for Mass Spectrometry*, 2010, **21**, 670–680.
17. A. Misharin, O. Silivra, F. Kjeldsen, and R. Zubarev, *Rapid Communications in Mass Spectrometry*, 2005, **19**, 2163–2171.

18. M. Toyoda, A. E. Giannakopoulos, A. W. Colburn, P. J. Derrick, *Rev. Sci. Instrum.* 2007, **78**, 074101.
19. J. M. Hettick, D. L. McCurdy, D. C. Barbacci, D. H. Russell, *Anal. Chem.* 2001, **73**, 5378–5386.
20. Yoon, S. H.; Chung, Y. J.; Kim, M. S. *J. Am. Soc. Mass Spectrom.* 2008, **19**, 645–655
21. R. Antoine, M. Broyer, J. Chamot-Rooke, C. Dedonder, C. Desfrancois, P. Dugourd, G. Grégoire, C. Jouvret, D. Onidas, P. Poulain, T. Tabarin, and G. van der Rest, *Rapid Communications in Mass Spectrometry*, 2006, **20**, 1648–1652.
22. S. Bari, O. Gonzalez-Magaña, G. Reitsma, J. Werner, S. Schippers, R. Hoekstra, and T. Schlathölder, *The Journal of Chemical Physics*, 2011, **134**, 024314.
23. O. González-Magaña, G. Reitsma, S. Bari, R. Hoekstra, T. Schlathölder, *Phys. Chem. Chem. Phys.* 2012, **14**, 4351–4354.
24. C. Brunet, R. Antoine, P. Dugourd, F. Canon, A. Giuliani, L. Nahon, *J. Am. Soc. Mass Spectrom.* 2012, **23**, 274–281.
25. L. Nahon, N. de Oliveira, G. A. Garcia, J.-F. Gil, B. Pilette, O. Marcouille, B. Lagarde, and F. Polack, *Journal of Synchrotron Radiation*, 2012, **19**, 508–520.
26. A. R. Milosavljević, C. Nicolas, J.-F. Gil, F. Canon, M. Réfrégiers, L. Nahon, and A. Giuliani, *Journal of Synchrotron Radiation*, 2012, **19**, 174–178.
27. A. R. Milosavljević, C. Nicolas, J.-F. Gil, F. Canon, M. Réfrégiers, L. Nahon, and A. Giuliani, *Nuclear Instruments and Methods in Physics Research Section B: Beam Interactions with Materials and Atoms*, 2012, **279**, 34–36.
28. M. Strohalm, D. Kavan, P. Novák, M. Volný, and V. Havlíček, *Analytical Chemistry*, 2010, **82**, 4648–4651.
29. B. A. Budnik and R. A. Zubarev, *Chemical Physics Letters*, 2000, **316**, 19–23.
30. A. Giuliani, A. R. Milosavljević, K. Hinsén, F. Canon, C. Nicolas, M. Réfrégiers, and L. Nahon, *Angewandte Chemie International Edition*, 2012, **51**, 9552–9556.
31. A. R. Milosavljević, V. Z. Cerovski, F. Canon, L. Nahon, and A. Giuliani, *Angewandte Chemie International Edition*, 2013, **52**, 7286–7290.
32. D. Close, *J Phys Chem A*, 2011, **115**, 2900–2912.
33. P. H. Cannington and N. S. Ham, *Journal of Electron Spectroscopy and Related Phenomena*, 1983, **32**, 139–151.
34. R. A. Zubarev and H. Yang, *Angewandte Chemie International Edition*, 2010, **49**, 1439–1441.
35. C. Brunet, R. Antoine, P. Dugourd, D. Duflot, F. Canon, A. Giuliani, and L. Nahon, *New J. Phys.*, 2013, **15**, 063024.
36. J. P. Reilly, *Mass spectrometry Reviews*, 2009, **28**, 425–447.
37. L. Zhang and J. P. Reilly, *Journal of the American Society for Mass Spectrometry*, 2009, **20**, 1378–1390.
38. Z. Guan, N. Kelleher, P. O'Connor, D. Aaserud, D. Little, and F. McLafferty, *International Journal of Mass Spectrometry and Ion Processes*, 1996, **157**, 357–364.
39. T. Goto, A. Ikehata, Y. Morisawa, and Y. Ozaki, *J Phys Chem A*, 2013, **117**, 2517–2528.
40. H. J. Cooper, R. R. Hudgins, K. Håkansson, and A. G. Marshall, *Journal of the American Society for Mass Spectrometry*, 2002, **13**, 241–249.
41. M. L. Nielsen, B. A. Budnik, K. F. Haselmann, and R. A. Zubarev, *International Journal of Mass Spectrometry*, 2003, **226**, 181–187.
42. J. Laskin, Z. Yang, C. M. D. Ng, and I. K. Chu, *Journal of the American Society for Mass Spectrometry*, 2010, **21**, 511–521.
43. M. Schwell, Y. Bénilan, N. Fray, M.-C. Gazeau, E. Es-Sebbar, G. A. Garcia, L. Nahon, N. Champion, and S. Leach, *Chemical Physics*, 2012, **393**, 107–116.
44. G. Aravind, B. Klærke, J. Rajput, Y. Toker, L. H. Andersen, A. V. Bochenkova, R. Antoine, J. Lemoine, A. Racaud, and P. Dugourd, *The Journal of Chemical Physics*, 2012, **136**, 014307.
45. M. Pérot, B. Lucas, M. Barat, J. A. Fayeton, and C. Jouvret, *J Phys Chem A*, 2010, **114**, 3147–3156.
46. B. Lucas, M. Barat, J. A. Fayeton, C. Jouvret, P. Çarçabal, and G. Grégoire, *Chemical Physics*, 2008, **347**, 324–330.
47. R. Parthasarathi, Y. He, J. P. Reilly, and K. Raghavachari, *Journal of the American Chemical Society*, 2010, **132**, 1606–1610.
48. L. Serrano-Andrés and B. O. Roos, *Journal of the American Chemical Society*, 1996, **118**, 185–195.
49. L. Serrano-Andrés and M. Fülcher, *Journal of the American Chemical Society*, 1996, **118**, 12190–12199.
50. E. Gindensperger, A. Haegy, C. Daniel, and R. Marquardt, *Chemical Physics*, 2010, **374**, 104–110.
51. G. Grégoire, C. Jouvret, C. Dedonder, and A. L. Sobolewski, *Journal of the American Chemical Society*, 2007, **129**, 6223–6231.
52. B. M. Bulheller, A. J. Miles, B. A. Wallace, and J. D. Hirst, *Journal of Physical Chemistry B*, 2008, **112**, 1866–1874.
53. L. Serrano-Andrés and M. P. Fülcher, *Journal of Physical Chemistry B*, 2001, **105**, 9323–9330.
54. L. Serrano-Andrés and M. P. Fülcher, *Journal of the American Chemical Society*, 1998, **120**, 10912–10920.
55. N. A. Besley, M. T. Oakley, A. J. Cowan, and J. D. Hirst, *Journal of the American Chemical Society*, 2004, **126**, 13502–13511.
56. R. Improta, L. Vitagliano, and L. Esposito, *PLoS ONE*, 2011, **6**, e24533.
57. B. A. Wallace, *Journal of Synchrotron Radiation*, 2000, **7**, 289–295.
58. D. T. Clarke and G. R. Jones, *Biochemistry*, 1999, **38**, 10457–10462.
59. L. Serrano-Andrés and M. Fülcher, *Journal of the American Chemical Society*, 1996, **118**, 12200–12206.
60. P. Limão-Vieira, S. Eden, P. A. Kendall, N. J. Mason, and S. V. Hoffmann, *Chemical Physics Letters*, 2002, **366**, 343–349.
61. M. B. Williams, P. Campuzano-Jost, D. D. Riemer, C. Tatum, and A. J. Hynes, *Journal of Photochemistry and Photobiology A: Chemistry*, 2005, **171**, 77–82.
62. M. Thompson, W. Cui, and J. Reilly, *Angewandte Chemie International Edition*, 2004, **43**, 4791–4794.
63. M. B. Robin, *Higher excited states of polyatomic molecules*, 1985.
64. X.-B. Chen, W.-H. Fang, and D.-C. Fang, *Journal of the American Chemical Society*, 2003, **125**, 9689–9698.
65. C. Kalcic, T. Gunaratne, A. Jones, M. Dantus, and G. Reid, *Journal of the American Chemical Society*, 2009, **131**, 940–942.
66. C. L. Kalcic, G. E. Reid, V. V. Lozovoy, and M. Dantus, *Journal of Physical Chemistry A*, 2012, **116**, 2764–2774.
67. J. Laskin, Z. Yang, C. Lam, and I. Chu, *Analytical Chemistry*, 2007, **79**, 6607–6614.
68. F. Wien, A. J. Miles, J. G. Lees, S. Vørnning Hoffmann, and B. A. Wallace, *Journal of Synchrotron Radiation*, 2005, **12**, 517–523.